Blind Joint DOA and Polarization Estimation for Polarization Sensitive Coprime Planar Arrays via a Fast-Convergence Quadrilinear Decomposition Approach

XU Xiong[1], *SHEN Jinqing*[1,2], *ZHU Beizuo*[1,2], *ZHANG Xiaofei*[1,2*]

1. State Key Laboratory of Complex Electromagnetic Environment Effects (CEMEE) on Electronics and Information System, Luoyang 471003, P.R.China;

2. College of Electronic and Information Engineering, Nanjing University of Aeronautics and Astronautics, Nanjing 211106, P.R.China

(Received 20 December 2019; revised 18 June 2020; accepted 18 September 2020)

Abstract: The problem of joint direction of arrival (DOA) and polarization estimation for polarization sensitive coprime planar arrays (PS-CPAs) is investigated, and a fast-convergence quadrilinear decomposition approach is proposed. Specifically, we first decompose the PS-CPA into two sparse polarization sensitive uniform planar subarrays and employ propagator method (PM) to construct the initial steering matrices separately. Then we arrange the received signals into two quadrilinear models so that the potential DOA and polarization estimates can be attained via quadrilinear alternating least square (QALS). Subsequently, we distinguish the true DOA estimates from the approximate intersecting estimations of the two subarrays in view of the coprime feature. Finally, the polarization estimates paired with DOA can be obtained. In contrast to the conventional QALS algorithm, the proposed approach can remarkably reduce the computational complexity without degrading the estimation performance. Simulations demonstrate the superiority of the proposed fast-convergence approach for PS-CPAs.

Key words: polarization sensitive arrays; coprime planar arrays; direction of arrival (DOA) estimation; polarization estimation; quadrilinear decomposition; fast convergence

CLC number: TN925 **Document code:** A **Article ID:** 1005-1120(2020)05-0778-09

0 Introduction

Polarization characteristic of electromagnetic wave has played an important role in target detection and recognition[1]. Polarization sensitive arrays (PSAs) have been widely utilized in vital applications such as radar, navigation and wireless communications[2]. Compared with the traditional arrays with scalar sensors, PSAs with electromagnetic vector sensors (EMVSs) offer desirable improvements in array performance[3]. Various angle-polarization estimation methods for PSAs have been proposed[4-5], including multiple signal classification (MUSIC) algorithm[6], estimating signal parameters via rotational invariance techniques (ESPRIT)[7], etc. However, the compact structures of most PSAs with inter-element spacing no more than half-wavelength restrict the resolution.

Recently, the coprime arrays[8-11], a newly emerged typical sparse array structure, have attracted more and more concerns for their inherent advantages over the uniform arrays, e.g. enlarged array aperture, increased degrees of freedom and improved estimation performance. Varieties of methods have been developed for conducting direction of arrival (DOA) estimation for coprime arrays. In Ref. [9], a representative method of phase ambiguity elimination is proposed. The traditional MUSIC

*Corresponding author, E-mail address: zhangxiaofei@nuaa.edu.cn.

How to cite this article: XU Xiong, SHEN Jinqing, ZHU Beizuo, et al. Blind joint DOA and polarization estimation for polarization sensitive coprime planar arrays via a fast-convergence quadrilinear decomposition approach[J]. Transactions of Nanjing University of Aeronautics and Astronautics, 2020, 37(5): 778-786.

http://dx.doi.org/10.16356/j.1005-1120.2020.05.012

algorithm for uniform arrays is extended to coprime planar arrays in Ref. [10], whereas the two-dimensional (2D) total spectral search (TSS) brings a tremendous amount of computing. In order to reduce the computational burden, Ref. [11] converts the 2D TSS into one-dimensional partial spectral search.

However, the existing studies mainly take the scalar coprime arrays into account, where the significant polarization characteristic of the electromagnetic wave is neglected. Moreover, the subspace-based methods usually omit the structural characteristic of received signals. Tensor algebra-based tools are effective in improving the estimation performance due to its excellent anti-noise capacity[12]. Parallel factor (PARAFAC) technique[13], a typical tensor-based decomposition, has been turned out to be computationally efficient in multi-parameter estimation by factorizing the tensor data and employing the least squares (LS) estimation. Quadrilinear decomposition algorithm[14], has been successfully applied in DOA and polarization estimation. Unfortunately, the conventional quadrilinear decomposition-based algorithm suffers from heavy computational burden.

In this paper, we investigate the problem of joint multi-parameter estimation for polarization sensitive coprime planar arrays (PS-CPAs) and derive a fast-convergence quadrilinear decomposition approach. The main contributions are as follows: (1) We take the polarization sensitive coprime planar arrays into consideration, which can take full advantages of coprime arrays and polarization sensitive arrays to enhance the array performance and achieve better engineering applicability. (2) We develop a connection between the DOA and polarization estimation problem for PS-CPAs and quadrilinear decomposition problem, which utilizes the structural characteristic of received signal data and thereby construct it as two quadrilinear models. (3) We propose a fast-convergence quadrilinear decomposition approach for PS-CPAs, where an initial estimation with PM is exploited to construct the initial matrices and significantly reduces the complexity. Furthermore, the proposed approach outperforms ESPRIT and PM in parameter estimation.

1 Data Model

Suppose that a PS-CPA configuration consists of two uniform planar subarrays (UPAs) with $M_i \times M_i$ ($i=1,2$) crossed short dipoles. The distances of adjacent sensors of the subarray with $M_1 \times M_1$ sensors is $d_1 = M_2\lambda/2$, while the other with $M_2 \times M_2$ sensors is $d_2 = M_1\lambda/2$, where M_1 and M_2 are coprime integers and λ is the wavelength. The two subarrays share the same element at the origin of coordinates. A PS-CPA configuration is displayed in Fig.1 as an example.

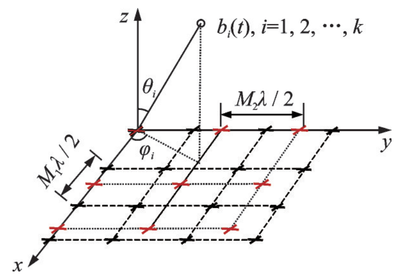

Fig.1 PS-CPA configuration with $M_1=3$ and $M_2=4$

Assume K ($K < \min\{M_1^2, M_2^2\}$) far-field uncorrelated signals impinge on the PS-CPA from $\{(\theta_k, \varphi_k) | k=1,2,\cdots,K\}$. Define that $\theta_k \in [0, \pi/2]$ is the elevation angle, $\varphi_k \in [0, \pi]$ the azimuth angle. $\gamma_k \in [0, \pi/2]$ and $\eta_k \in [-\pi, \pi]$ are polarization parameters of the k-th signal. Define a transformation as $u_k = \sin\theta_k \cos\varphi_k$, $v_k = \sin\theta_k \sin\varphi_k$ for simplification.

Considering that the PS-CPA can be decomposed into two polarization sensitive uniform planar arrays (PS-UPAs), we process the signal data with the two PS-UPAs separately and elaborate on the proposed approach with the subarray of $M_i \times M_i$ ($i=1,2$) crossed short dipoles.

The output of the i-th subarray can be presented by[5]

$$\boldsymbol{X}_i = [\boldsymbol{a}_{i,1} \otimes \boldsymbol{s}_1, \boldsymbol{a}_{i,2} \otimes \boldsymbol{s}_2, \cdots, \boldsymbol{a}_{i,K} \otimes \boldsymbol{s}_K] \boldsymbol{B}^{\mathrm{T}} + \boldsymbol{N}_i = (\boldsymbol{A}_i \odot \boldsymbol{S}) \boldsymbol{B}^{\mathrm{T}} + \boldsymbol{N}_i = (\boldsymbol{A}_{i,y} \odot \boldsymbol{A}_{i,x} \odot \boldsymbol{S}) \boldsymbol{B}^{\mathrm{T}} + \boldsymbol{N}_i \tag{1}$$

where $\boldsymbol{B} = [\boldsymbol{b}_1, \boldsymbol{b}_2, \cdots, \boldsymbol{b}_K] \in \boldsymbol{C}^{L \times K}$ represents the signal matrix, $\boldsymbol{b}_k = [b_k(1), b_k(2), \cdots, b_k(L)]^{\mathrm{T}}$; L the number of snapshots; $\boldsymbol{N}_i \in \boldsymbol{C}^{2M_i^2 \times L}$ the received noise which is zero-mean white Gaussian independent with signals. $\boldsymbol{A}_i=[\boldsymbol{a}_{i,1},\boldsymbol{a}_{i,2},\cdots,\boldsymbol{a}_{i,K}]\in\boldsymbol{C}^{M_i^2\times K}$ the steering matrix, where $\boldsymbol{a}_{i,k}=\boldsymbol{a}_{i,y}(v_k)\otimes\boldsymbol{a}_{i,x}(u_k)$ is the steering vector; $\otimes$ and $\odot$ denote the Kronecker product and the Khatri-Rao product, respectively; $(\cdot)^{\mathrm{T}}$ is the operation of transpose; $\boldsymbol{A}_{i,x}=[\boldsymbol{a}_{i,x_1},\boldsymbol{a}_{i,x_2},\cdots,\boldsymbol{a}_{i,x_K}]$ and $\boldsymbol{A}_{i,y}=[\boldsymbol{a}_{i,y_1},\boldsymbol{a}_{i,y_2},\cdots,\boldsymbol{a}_{i,y_K}]$ represent the steering matrices corresponding to the x- and y-axis direction, respectively. And $\boldsymbol{a}_{i,x}(u_k)$ and $\boldsymbol{a}_{i,y}(v_k)$ are the steering vectors and can be expressed as

$$\boldsymbol{a}_{i,x}(u_k)=[1,\mathrm{e}^{-\mathrm{j}2\pi d_i u_k/\lambda},\cdots,\mathrm{e}^{-\mathrm{j}2\pi(M_i-1)d_i u_k/\lambda}]^{\mathrm{T}} \tag{2}$$

$$\boldsymbol{a}_{i,y}(v_k)=[1,\mathrm{e}^{-\mathrm{j}2\pi d_i v_k/\lambda},\cdots,\mathrm{e}^{-\mathrm{j}2\pi(M_i-1)d_i v_k/\lambda}]^{\mathrm{T}} \tag{3}$$

and $\boldsymbol{S}=[\boldsymbol{s}_1,\boldsymbol{s}_2,\cdots,\boldsymbol{s}_K]^{\mathrm{T}}\in\boldsymbol{C}^{2\times K}$ is the polarization matrix, where the polarization vector $\boldsymbol{s}_k$ is

$$\boldsymbol{s}_k=\begin{bmatrix}\cos\theta_k\cos\varphi_k & -\sin\varphi_k\\ \cos\theta_k\sin\varphi_k & \cos\varphi_k\end{bmatrix}\begin{bmatrix}\sin\gamma_k\mathrm{e}^{\mathrm{j}\eta_k}\\ \cos\gamma_k\end{bmatrix} \tag{4}$$

Eq.(1) can be written as

$$\boldsymbol{X}_i=\begin{bmatrix}\boldsymbol{X}_{i,1,1}\\ \boldsymbol{X}_{i,1,2}\\ \vdots\\ \boldsymbol{X}_{i,M_i,N_i}\end{bmatrix}=\begin{bmatrix}\boldsymbol{S}\boldsymbol{D}_1(\boldsymbol{A}_{i,x})\boldsymbol{D}_1(\boldsymbol{A}_{i,y})\\ \boldsymbol{S}\boldsymbol{D}_1(\boldsymbol{A}_{i,x})\boldsymbol{D}_2(\boldsymbol{A}_{i,y})\\ \vdots\\ \boldsymbol{S}\boldsymbol{D}_{M_i}(\boldsymbol{A}_{i,x})\boldsymbol{D}_{N_i}(\boldsymbol{A}_{i,y})\end{bmatrix}\boldsymbol{B}^{\mathrm{T}}+\boldsymbol{N}_i \tag{5}$$

where $N_i=M_i$ in the subarrays of PS-CPA considered; $\boldsymbol{D}_m(\boldsymbol{A})$ produces a diagonal matrix formed by the m-th row of $\boldsymbol{A}$. To describe the quadrilinear model more exhaustively, we use the subarray with $M_i\times N_i$ EMVSs to illustrate it. $\boldsymbol{X}_{i,m,n}$ in Eq.(5) can be denoted as the quadrilinear model[14]

$$x_{i,m,n,p,l}=\sum_{k=1}^{K}a_{i,m,k}a_{i,n,k}s_{p,k}b_{l,k}+\boldsymbol{n}_{i,m,n,p,l}$$
$$m=1,\cdots,M_i;n=1,\cdots,N_i;p=1,2;l=1,\cdots,L \tag{6}$$

where $a_{i,m,k}$, $a_{i,n,k}$ represent the (m,k)-th, (n,k)-th items in $\boldsymbol{A}_{i,x}$, $\boldsymbol{A}_{i,y}$, respectively; $s_{p,k}$ stands for the (p,k)-th element of $\boldsymbol{S}$ is; $b_{l,k}$ the (l,k)-th element of $\boldsymbol{B}$; and $\boldsymbol{n}_{i,m,n,p,l}$ the (m,n,p,l)-th element of $\boldsymbol{N}_i$ which is regarded as a four-array matrix. The other rearranged matrices can be derived from the structural characteristics of the quadrilinear model as

$$\boldsymbol{U}_i=(\boldsymbol{S}\odot\boldsymbol{A}_{i,x}\odot\boldsymbol{B})\boldsymbol{A}_{i,y}^{\mathrm{T}}+\boldsymbol{N}_{i,u} \tag{7}$$

$$\boldsymbol{V}_i=(\boldsymbol{B}\odot\boldsymbol{S}\odot\boldsymbol{A}_{i,y})\boldsymbol{A}_{i,x}^{\mathrm{T}}+\boldsymbol{N}_{i,v} \tag{8}$$

$$\boldsymbol{W}_i=(\boldsymbol{A}_{i,y}\odot\boldsymbol{B}\odot\boldsymbol{A}_{i,x})\boldsymbol{S}^{\mathrm{T}}+\boldsymbol{N}_{i,w} \tag{9}$$

2 The Proposed Approach

To accelerate convergence and reduce complexity effectively, instead of initializing the loading matrices randomly like the conventional QALS method, we first make an initial estimation with PM to construct the initial $\boldsymbol{A}_{i,x}$ and $\boldsymbol{A}_{i,y}$, and then iteratively update the four loading matrices in turn according to QALS until the convergence. The coprime relationship between the two subarrays is exploited to remove the ambiguity. Finally, the polarization parameters can be obtained with the previous estimates.

2.1 Initialization with PM

Define $\boldsymbol{G}_i=\boldsymbol{A}_i\odot\boldsymbol{S}$ and partition $\boldsymbol{G}_i\in\boldsymbol{C}^{2M_i^2\times K}$ into $\boldsymbol{G}_i=[\boldsymbol{G}_{i,1}^{\mathrm{T}},\boldsymbol{G}_{i,2}^{\mathrm{T}}]^{\mathrm{T}}$. $\boldsymbol{G}_{i,1}\in\boldsymbol{C}^{K\times K}$ is nonsingular and $\boldsymbol{G}_{i,2}\in\boldsymbol{C}^{(2M_i^2-K)\times K}$, where $(\cdot)^{\mathrm{H}}$ is the conjugate transpose operation. There exists a linear transformation $\boldsymbol{P}_i^{\mathrm{H}}\boldsymbol{G}_{i,1}=\boldsymbol{G}_{i,2}$, where $\boldsymbol{P}_i\in\boldsymbol{C}^{K\times(2M_i^2-K)}$ is defined as the propagator matrix and can be calculated by[15]

$$\hat{\boldsymbol{P}}_i=(\boldsymbol{X}_{i,1}\boldsymbol{X}_{i,1}^{\mathrm{H}})^{-1}\boldsymbol{X}_{i,1}\boldsymbol{X}_{i,2}^{\mathrm{H}} \tag{10}$$

where $\boldsymbol{X}_{i,1}$ means the first K rows of $\boldsymbol{X}_i$; and $\boldsymbol{X}_{i,2}$ the remaining rows. Define

$$\hat{\boldsymbol{P}}_{i,c}=[\boldsymbol{I}_K\ \hat{\boldsymbol{P}}_i^{\mathrm{H}}]^{\mathrm{T}} \tag{11}$$

where $\hat{\boldsymbol{P}}_{i,c}\in\boldsymbol{C}^{2M_i^2\times K}$; and $\boldsymbol{I}_K\in\boldsymbol{C}^{K\times K}$ is an identity matrix. In the noise-free case, $\boldsymbol{G}_i=\hat{\boldsymbol{P}}_{i,c}\boldsymbol{G}_{i,1}$. $\hat{\boldsymbol{P}}_{i,c}$ can be written as

$$\hat{\boldsymbol{P}}_{i,c}=\boldsymbol{G}_i\boldsymbol{G}_{i,1}^{-1}=\begin{bmatrix}\boldsymbol{S}\\ \boldsymbol{S}\boldsymbol{\Phi}_{i,p}\\ \vdots\\ \boldsymbol{S}\boldsymbol{\Phi}_{i,p}^{M_i^2-1}\end{bmatrix}\boldsymbol{G}_{i,1}^{-1} \tag{12}$$

where $\boldsymbol{\Phi}_{i,p}=\mathrm{diag}\{p_{i,1},p_{i,2},\cdots,p_{i,K}\}$ and $p_{i,k}=\mathrm{e}^{-\mathrm{j}2\pi d_i v_k/\lambda}$. $\mathrm{diag}(\cdot)$ represents a diagonal matrix consisting of the included elements as diagonal elements. Then we have $\boldsymbol{P}_{i,b}=\boldsymbol{P}_{i,a}\boldsymbol{G}_{i,1}\boldsymbol{\Phi}_{i,p}\boldsymbol{G}_{i,1}^{-1}$ by partitioning $\hat{\boldsymbol{P}}_{i,c}$, where $\boldsymbol{P}_{i,a}$ and $\boldsymbol{P}_{i,b}$ are the first $2M_i(M_i-1)$ rows and the last $2M_i(M_i-1)$ rows of the matrix $\hat{\boldsymbol{P}}_{i,c}$, respectively. The initial estimates $\hat{v}_{i,k_0}$ of $\hat{v}_{i,k}$ can be sequentially achieved, which refers to the k-th eigenvalue of $\boldsymbol{P}_{i,a}^{\dagger}\boldsymbol{P}_{i,b}$, where $\|\cdot\|^{\dagger}$ stands for pseudo-inverse. Meanwhile, we can obtain the eigenvectors $\hat{\boldsymbol{G}}_{i,1}$. In the noise-free case, $\hat{\boldsymbol{G}}_{i,1}=\boldsymbol{G}_{i,1}\boldsymbol{\Pi}$, $\hat{\boldsymbol{\Phi}}_{i,p}=\boldsymbol{\Pi}\boldsymbol{\Phi}_{i,p}\boldsymbol{\Pi}^{-1}$, where $\boldsymbol{\Pi}$ is a permutation matrix, and $\boldsymbol{\Pi}^{-1}=\boldsymbol{\Pi}$. Accordingly, the estimate of $\boldsymbol{G}_i$ is

$$\hat{G}_i = \hat{P}_{i,c}\hat{G}_{i,1} = G_i \boldsymbol{\Pi} \tag{13}$$

Reconstructing $\hat{G}_i$ by rows reorganization, we have

$$\hat{G}_{i,r} = G_{i,r}\boldsymbol{\Pi} = \begin{bmatrix} S \\ S\boldsymbol{\Phi}_{i,q} \\ \vdots \\ S\boldsymbol{\Phi}_{i,q}^{M_i^2-1} \end{bmatrix} \boldsymbol{\Pi} \tag{14}$$

where $\boldsymbol{\Phi}_{i,q} = \mathrm{diag}\{q_{i,1}, q_{i,2}, \cdots, q_{i,K}\}$ and $q_{i,k} = \mathrm{e}^{-\mathrm{j}2\pi d_i u_k/\lambda}$. Similarly, we achieve the initial estimates $\hat{u}_{i,k_0}$ of $\hat{u}_{i,k}$ by partitioning $\hat{G}_{i,r}$ and get $\hat{\boldsymbol{\Phi}}_{i,q} = \boldsymbol{\Pi}\boldsymbol{\Phi}_{i,q}\boldsymbol{\Pi}^{-1}$.

Note that $\hat{\boldsymbol{\Phi}}_{i,p}$ and $\hat{\boldsymbol{\Phi}}_{i,q}$ have the same permutation ambiguity, which means that $\hat{u}_{i,k_0}$ and $\hat{v}_{i,k_0}$ are automatically paired. To decrease computational complexity, here we only initialize $A_{i,x}$, $A_{i,y}$ with $\hat{u}_{i,k_0}, \hat{v}_{i,k_0}$.

2.2 Quadrilinear decomposition

Herein, we initialize the steering matrices $A_{i,x}$ and $A_{i,y}$ with $\hat{u}_{i,k_0}$ and $\hat{v}_{i,k_0}$ to speed the convergence. And the initial polarization matrix S and signal matrix B are constructed randomly.

According to Eq.(1), the costing function of B in the quadrilinear model is

$$\min_{A_{i,x},A_{i,y},S,B} \left\| \tilde{X}_i - \left(A_{i,y} \odot A_{i,x} \odot S\right) B^{\mathrm{T}} \right\|_{\mathrm{F}} \tag{15}$$

where $\tilde{X}_i$ represents the noisy signal; $\|\cdot\|_{\mathrm{F}}$ the Frobenius norm. And the LS update for B is

$$\hat{B}^{\mathrm{T}} = (\hat{A}_{i,y} \odot \hat{A}_{i,x} \odot \hat{S})^{\dagger} \tilde{X}_i \tag{16}$$

where $\hat{A}_{i,x}$, $\hat{A}_{i,y}$ and $\hat{S}$ represent the previously obtained estimates of $A_{i,x}$, $A_{i,y}$ and S, respectively. According to the symmetry of the quadrilinear model, the LS fitting for $A_{i,y}$ is

$$\min_{A_{i,x},A_{i,y},S,B} \left\| \tilde{U}_i - (S \odot A_{i,x} \odot B) A_{i,y}^{\mathrm{T}} \right\|_{\mathrm{F}} \tag{17}$$

where $\tilde{U}_i$ is the noisy signal. And the LS update for $A_{i,y}$ can be expressed as

$$A_{i,y}^{\mathrm{T}} = (\hat{S} \odot \hat{A}_{i,x} \odot \hat{B})^{\dagger} \tilde{U}_i \tag{18}$$

where $\hat{S}$, $\hat{A}_{i,x}$ and $\hat{B}$ are estimated in the previous update process.

According to Eq.(8), the LS fitting for $A_{i,x}$ is

$$\min_{A_{i,x},A_{i,y},S,B} \left\| \tilde{V}_i - (B \odot S \odot A_{i,y}) A_{i,x}^{\mathrm{T}} \right\|_{\mathrm{F}} \tag{19}$$

where $\tilde{V}_i$ represents the noisy signal. Then the updated estimates of $A_{i,x}$ based on LS is

$$A_{i,x}^{\mathrm{T}} = (\hat{B} \odot \hat{S} \odot \hat{A}_{i,y})^{\dagger} \tilde{V}_i \tag{20}$$

where $\hat{B}$, $\hat{S}$ and $\hat{A}_{i,y}$ are previously estimated.

In a similar way, the LS fitting for S is

$$\min_{A_{i,x},A_{i,y},S,B} \left\| \tilde{W}_i - (A_{i,y} \odot B \odot A_{i,x}) S^{\mathrm{T}} \right\|_{\mathrm{F}} \tag{21}$$

where $\tilde{W}_i$ is the noisy signal. The LS update for S is

$$\hat{S}^{\mathrm{T}} = (\hat{A}_{i,y} \odot \hat{B} \odot \hat{A}_{i,x})^{\dagger} \tilde{W}_i \tag{22}$$

where $\hat{A}_{i,y}$, $\hat{B}$ and $\hat{A}_{i,x}$ are the previous estimats.

The sum of squared residuals (SSR) is defined as $\mathrm{SSR}_k = \sum_{r=1}^{2M_i}\sum_{l=1}^{L}\left|c_{rl}\right|^2$, where r, l represent the (r, l)-th elements of matrix $C = X_i - (A_i \odot S) B^{\mathrm{T}}$. The convergence rate is denoted as $\mathrm{SSR}_{\mathrm{rate}} = (\mathrm{SSR}_k - \mathrm{SSR}_{k-1}) / \mathrm{SSR}_{k-1}$. According to Eqs. (16), (18), (20) and (22), we repeatedly perform the updating process of $\hat{B}, \hat{A}_{i,x}, \hat{A}_{i,y}$ and $\hat{S}$ with LS until $\mathrm{SSR}_{\mathrm{rate}} < \varepsilon$, where ε is a certain small value[16].

Thereafter, we achieve the estimates as

$$\hat{B}_i'' = B_i \boldsymbol{\Pi}_i \boldsymbol{\Delta}_{i,1} + V_{i,1} \tag{23}$$

$$\hat{A}_{i,x}'' = A_{i,x} \boldsymbol{\Pi}_i \boldsymbol{\Delta}_{i,2} + V_{i,2} \tag{24}$$

$$\hat{A}_{i,y}'' = A_{i,y} \boldsymbol{\Pi}_i \boldsymbol{\Delta}_{i,3} + V_{i,3} \tag{25}$$

$$\hat{S}_i'' = \hat{S}_i \boldsymbol{\Pi}_i \boldsymbol{\Delta}_{i,4} + V_{i,4} \tag{26}$$

where $\boldsymbol{\Pi}_i$ represents a permutation matrix, which may lead to permutation ambiguity. And $\boldsymbol{\Delta}_{i,1}$, $\boldsymbol{\Delta}_{i,2}$, $\boldsymbol{\Delta}_{i,3}$, $\boldsymbol{\Delta}_{i,4}$ are the diagonal scaling matrices satisfying $\boldsymbol{\Delta}_{i,1}\boldsymbol{\Delta}_{i,2}\boldsymbol{\Delta}_{i,3}\boldsymbol{\Delta}_{i,4} = I_K$, which may lead to scale ambiguity. $V_{i,1}$, $V_{i,2}$, $V_{i,3}$ and $V_{i,4}$ represent the estimation errors. Since the permutation matrix $\boldsymbol{\Pi}_i$ in Eqs.(23)—(26) is the same, the permutation ambiguity makes no difference to parameters pairing. And the scale ambiguity can be resolved via normalization.

2.3 Least squares estimation

Define a_{i,x_k}'', a_{i,y_k}'' as the k-th columns of $\hat{A}_{i,x}''$, $\hat{A}_{i,y}''$, respectively. By normalizing a_{i,x_k}'', a_{i,y_k}'', we have

$$h_{i,u_k} = -\mathrm{angle}(a_{i,x}''(u_k)) = [0, 2\pi d_i u_k/\lambda, \cdots, 2\pi d_i(M_i-1) d u_k/\lambda]^{\mathrm{T}} \tag{27}$$

$$h_{i,v_k} = -\mathrm{angle}(a_{i,y}''(v_k)) = [0, 2\pi d_i v_k/\lambda, \cdots, 2\pi d_i(M_i-1) d v_k/\lambda]^{\mathrm{T}} \tag{28}$$

where angle(•) represents the operation of getting the phase angle. Then we use LS criterion to estimate u_k and v_k. The LS fitting is $Q_i c_{i,1} = h_{i,u_k}$ and $Q_i c_{i,2} = h_{i,v_k}$, where $c_{i,1} = [c_{i,1}', c_{i,1}'']^{\mathrm{T}}$, $c_{i,2} =$

$[c'_{i,2}, c''_{i,2}]^{\mathrm{T}}$ and

$$\boldsymbol{Q}_i=\begin{bmatrix}1 & 0\\ 1 & 2\pi d_i/\lambda\\ \vdots & \vdots\\ 1 & (M_i-1)2\pi d_i/\lambda\end{bmatrix} \tag{29}$$

According to LS criterion, we can obtain

$$\boldsymbol{c}_{i,1}=(\boldsymbol{Q}_i^{\mathrm{T}}\boldsymbol{Q}_i)^{-1}\boldsymbol{Q}_i^{\mathrm{T}}\hat{\boldsymbol{h}}_{i,u_k} \tag{30}$$

$$\boldsymbol{c}_{i,2}=(\boldsymbol{Q}_i^{\mathrm{T}}\boldsymbol{Q}_i)^{-1}\boldsymbol{Q}_i^{\mathrm{T}}\hat{\boldsymbol{h}}_{i,v_k} \tag{31}$$

Then the estimates of (u_k, v_k) can be achieved by

$$\hat{u}_{i,k}=\hat{c}''_{i,1} \tag{32}$$

$$\hat{v}_{i,k}=\hat{c}''_{i,2} \tag{33}$$

The $(\hat{u}_{i,k}, \hat{v}_{i,k})$ obtained in Eqs.(32), (33) is not necessarily true estimates as a result of the phase ambiguity problem caused by the enlarged element spacing.

2.4 Ambiguity elimination

We elucidate the generation and elimination method of phase ambiguity in this section.

Assume a single source impinges on the subarray with $M_i\times M_i$ EMVSs from the direction (θ_t, φ_t). Denote (θ_a, φ_a) as one of the ambiguous DOAs. The period of exponential function 2π implies that[11]

$$2\pi d_i(u_t-u_a)/\lambda=2k_{i,u}\pi \tag{34}$$

$$2\pi d_i(v_t-v_a)/\lambda=2k_{i,v}\pi \tag{35}$$

where $u_t=\sin\theta_t\cos\varphi_t$, $v_t=\sin\theta_t\sin\varphi_t$, $u_a=\sin\theta_a\cos\varphi_a$, $v_a=\sin\theta_a\sin\varphi_a$, $d_i=M_j\lambda/2(i,j\in\{1,2\}, i\neq j)$, $k_{i,u}\in\mathbf{Z}$, $k_{i,v}\in\mathbf{Z}$. Constraints $u_t, u_a\in[-1,1]$, $v_t, v_a\in[0,1]$, $0<u_t^2+v_t^2<1$, $0<u_a^2+v_a^2<1$ have to be satisfied.

From Eqs.(34), (35), we have

$$\frac{k_{1,u}}{M_2}=\frac{k_{2,u}}{M_1}, \frac{k_{1,v}}{M_2}=\frac{k_{2,v}}{M_1} \tag{36}$$

As M_1 and M_2 are coprime integers, there uniquely exist $k_{1,u}=k_{2,u}=0$ and $k_{1,v}=k_{2,v}=0$ making Eq.(36) valid, which reveals that the true DOA estimates can be uniquely distinguished from the intersecting estimations of the two subarrays. Since it is impractical for two subarrays containing completely coincident estimates, the closest ones are exactly required. Similar conclusions can be obtained in the case of multi-source.

2.5 Parameter estimation

With the unambiguous estimates defined as $\hat{u}_k^{\mathrm{fin}}, \hat{v}_k^{\mathrm{fin}}$, we obtain the true estimates $(\hat{\theta}_k, \hat{\varphi}_k)$ via

$$\hat{\theta}_k=\arcsin\left(\sqrt{(\hat{u}_k^{\mathrm{fin}})^2+(\hat{v}_k^{\mathrm{fin}})^2}\right) \tag{37}$$

$$\hat{\varphi}_k=\mathrm{angle}(\hat{u}_k^{\mathrm{fin}}+\mathrm{j}\hat{v}_k^{\mathrm{fin}}) \tag{38}$$

Since the ambiguity elimination process makes the pairing of $\hat{\boldsymbol{A}}''_{i,x}$, $\hat{\boldsymbol{A}}''_{i,y}$ and $\hat{\boldsymbol{S}}''_i$ invalid, we must determine the pairing of $\hat{\theta}_k, \hat{\varphi}_k$ and $\hat{\boldsymbol{S}}''_i$ before calculating the polarization parameters.

Construct $\hat{\boldsymbol{A}}_x^{\mathrm{fin}}$ with $\hat{\theta}_k$ and $\hat{\varphi}_k$. Considering that $\hat{\boldsymbol{u}}_i$, $\hat{\boldsymbol{A}}''_{i,x}$ and $\hat{\boldsymbol{S}}''_i$ are well paired, and so are $\hat{\boldsymbol{u}}^{\mathrm{fin}}$ and $\hat{\boldsymbol{A}}_x^{\mathrm{fin}}$, we just need to match the column vectors of $\hat{\boldsymbol{u}}^{\mathrm{fin}}$ and $\hat{\boldsymbol{u}}_i$, which essentially determines the pairing of $\hat{\boldsymbol{A}}_x^{\mathrm{fin}}$ and $\hat{\boldsymbol{S}}''_i$. Denote $\hat{u}_k^{\mathrm{fin}}(k=1,2,\cdots,K)$ as the k-th element of $\hat{\boldsymbol{u}}^{\mathrm{fin}}$, and $\hat{u}_{i,j}(j=1,2,\cdots,K)$ as the j-th element of $\hat{\boldsymbol{u}}_i$. Consequently, we ascertain the correspondence between the k and j by

$$j_k=\underset{j=1,2,\cdots,K}{\arg}\min\left\|\hat{u}_{i,j}-\hat{u}_k^{\mathrm{fin}}\right\|_2 \qquad k=1,2,\cdots,K \tag{39}$$

By this means, the pairing of $\hat{\boldsymbol{u}}^{\mathrm{fin}}$ and $\hat{\boldsymbol{u}}_i$ is achieved, so are $\hat{\theta}_k, \hat{\varphi}_k$ and $\hat{\boldsymbol{S}}''_i$. Define $\hat{\boldsymbol{S}}_i^{\mathrm{fin}}$ as the polarization matrix paired with $\hat{\theta}_k, \hat{\varphi}_k$. Since the two subarrays correspond to the same polarization matrix, we adopt an average operation as

$$\hat{\boldsymbol{s}}^{\mathrm{fin}}(\theta_k,\varphi_k,\gamma_k,\eta_k)=\frac{\hat{\boldsymbol{s}}_1^{\mathrm{fin}}(\theta_k,\varphi_k,\gamma_k,\eta_k)+\hat{\boldsymbol{s}}_2^{\mathrm{fin}})(\theta_k,\varphi_k,\gamma_k,\eta_k)}{2} \tag{40}$$

where $\hat{\boldsymbol{s}}_i^{\mathrm{fin}}(\theta_k,\varphi_k,\gamma_k,\eta_k)$ is the k-th column of $\hat{\boldsymbol{S}}_i^{\mathrm{fin}}$.

Subsequently, the polarization parameters can be determined from

$$\hat{\gamma}_k=\arctan(|\hat{\xi}_k|) \tag{41}$$

$$\hat{\eta}_k=\mathrm{angle}(\hat{\xi}_k) \tag{42}$$

where

$$\hat{\xi}_k=\frac{\hat{r}_k\cos\hat{\varphi}_k+\sin\hat{\varphi}_k}{\cos\hat{\theta}_k(\cos\hat{\varphi}_k-\hat{r}_k\sin\hat{\varphi}_k)} \tag{43}$$

and $\hat{r}_k=\hat{\boldsymbol{s}}_k^{\mathrm{fin}}(1)/\hat{\boldsymbol{s}}_k^{\mathrm{fin}}(2)$, $\hat{\boldsymbol{s}}_k^{\mathrm{fin}}(1)$ and $\hat{\boldsymbol{s}}_k^{\mathrm{fin}}(2)$ are the first and second elements of $\hat{\boldsymbol{s}}^{\mathrm{fin}}(\theta_k,\varphi_k,\gamma_k,\eta_k)$, respectively.

3 Performance Analysis

3.1 Convergence analysis

We compare the convergence performance of the proposed approach and the conventional QALS algorithm and illustrate the iteration times of the two subarrays in Fig.2, where we set SNR = 10 dB, $L = 100$. Define $\mathrm{DSSR} = \mathrm{SSR}_n - \mathrm{SSR}_c$, where SSR_n denotes the value of SSR corresponding to the n-th iteration and SSR_c the value of SSR at convergence.

It is explicitly indicated in Fig.2 that the proposed approach requires fewer iterations to converge than the conventional QALS algorithm. A faster convergence speed can lead to a lower computational complexity.

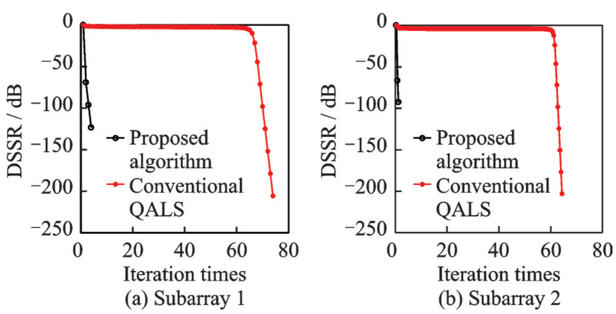

Fig.2 Convergence comparison of different algorithms

3.2 Complexity analysis

As the two subarrays of the PS-CPA possess the similar complexity form, the complexity calculation of the subarray with $M_i \times M_i$ sensors of our approach is shown as follows. The initialization with PM costs about $O(2K^2L + 3M_i(M_i - 1)K^2 + 3M_i(M_i - 1)K^2 + 5K^3 + (2M_i^2 - K)KL)$ $(i = 1, 2)$. Each iteration of QALS needs $O(K^2(2M_i^2 + M_i^2L + 4M_iL + 2M_i + L + 2) + 4K^3 + 8M_i^2KL)$. We list the complexity of the proposed approach and the conventional QALS algorithm in Table 1, where n_1 and n_2 are the number of iterations of the former and the latter, respectively.

Fig.3 displays the complexity comparison between PM and each iteration of QALS in the PS-CPA. We can conclude that although PM process is involved in initialization, the complexity of PM is lower than that of one iteration of QALS. Fig.4 displays the complexity comparison versus snapshots, where $K = 2$, $n_1 = 5$, $n_2 = 100$. It is observed from Figs.3, 4 that the proposed approach can reduce the complexity remarkably.

Table 1 Computational complexities of different algorithms

Algorithm	Computational complexity
The proposed approach	$O(2K^2L + 3M_i(M_i - 1)K^2 + 5K^3 + 3M_i(M_i - 1)K^2 + (2M_i^2 - K)KL + n_1(K^2(2M_i^2 + M_i^2L + 4M_iL + 2M_i + L + 2) + 4K^3 + 8M_i^2KL))$
Conventional QALS algorithm	$O(n_2(K^2(2M_i^2 + M_i^2L + 4M_iL + 2M_i + L + 2) + 4K^3 + 8M_i^2KL))$

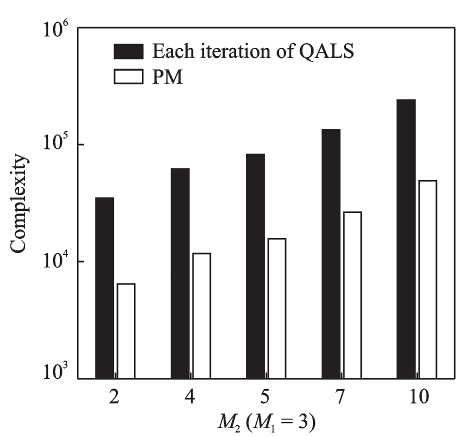

Fig.3 Complexity comparison between PM and each iteration of QALS in the PS-CPA

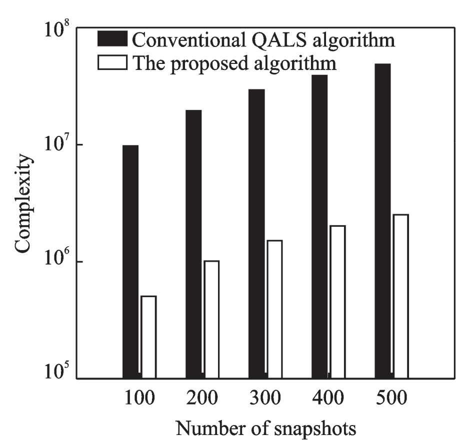

Fig.4 Complexity comparison of different snapshots between the proposed algorithm and the conventional QALS algorithm

3.3 Advantages

(1) The proposed approach achieves a fast convergence by employing PM as the initialization, which remarkably reduces the computational complexity.

(2) The proposed approach obtains the same parameter estimation performance as the conventional QALS algorithm but owns much lower computational burden, and outperforms PM and ESPRIT.

(3) The proposed approach in PS-CPA has a higher estimation accuracy than that in PS-UPA, owing to the larger array aperture.

4 Simulation Results

In this section, we perform 500 Monte-Carlo simulations to evaluate the parameter estimation performance. The root mean square error (RMSE) is defined by

$$\mathrm{RMSE}=\sqrt{\frac{1}{500K}\sum_{l=1}^{500}\sum_{k=1}^{K}(\alpha_k-\hat{\alpha}_{k,l})^2} \tag{44}$$

where $\hat{\alpha}_{k,l}$ is the estimate of DOA/polarization parameter corresponding to the k-th signal in the l-th simulation.

Suppose that $K=2$ signals impinge on the PS-CPA from $(\theta_1,\varphi_1)=(10°,30°)$, $(\theta_2,\varphi_2)=(20°,40°)$, and their corresponding polarization parameters are $(\gamma_1,\eta_1)=(7°,15°)$, $(\gamma_2,\eta_2)=(17°,25°)$.

4.1 Parameter estimation results

We examine the validity of the proposed approach and the scatter plots of parameter estimation is shown in Fig.5, where $M_1=4$, $M_2=5$, $L=200$ and SNR $=20$ dB. As illustrated in Fig.5, the approach is effective in estimating multi-parameters.

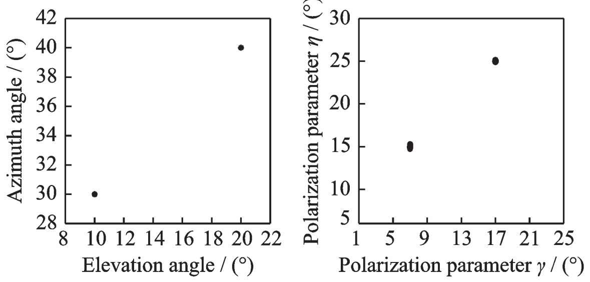

(a) Scatter plot of elevation angle and azimuth angle (b) Scatter plot of polarization γ and η

Fig.5 Estimation results of the proposed approach

4.2 RMSE comparison of different algorithms

We present the parameter estimation performance comparison of the proposed approach, the conventional QALS, ESPRIT, PM algorithms and the Cramer-Rao Bound[17] in Fig.6, where $M_1=7$, $M_2=9$ and $L=300$. It is clear from Fig.6 that the proposed approach has the same estimation performance as the conventional QALS algorithm but with a faster convergence, which shows that the proposed approach can guarantee estimation accuracy while reducing complexity effectively. By contrast, the proposed approach outperforms ESPRIT and PM, as it utilizes the structural characteristic of received signal and applies the quadrilinear alternating least square method.

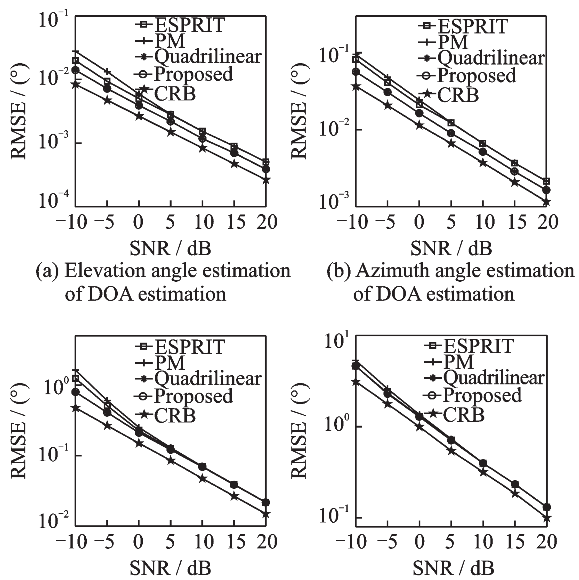

(a) Elevation angle estimation of DOA estimation (b) Azimuth angle estimation of DOA estimation
(c) Polarization γ estimation of polarization estimation (d) Polarization η estimation of polarization estimation

Fig.6 Parameter estimation performance of different algorithms

4.3 RMSE comparison with different arrays

We give the RMSE results of the proposed approach in PS-CPA and PS-UPA in Fig.7 to compare array performance, where $M_1=4$, $M_2=5$, $L=300$. Consider a PS-UPA with 5×8 sensors so that the two arrays have the same number of elements for fair. As depicted in Fig.7, the approach in PS-CPA has superior estimation performance to that in PS-UPA, as the PS-CPA enables a larger array aperture with the same number of elements.

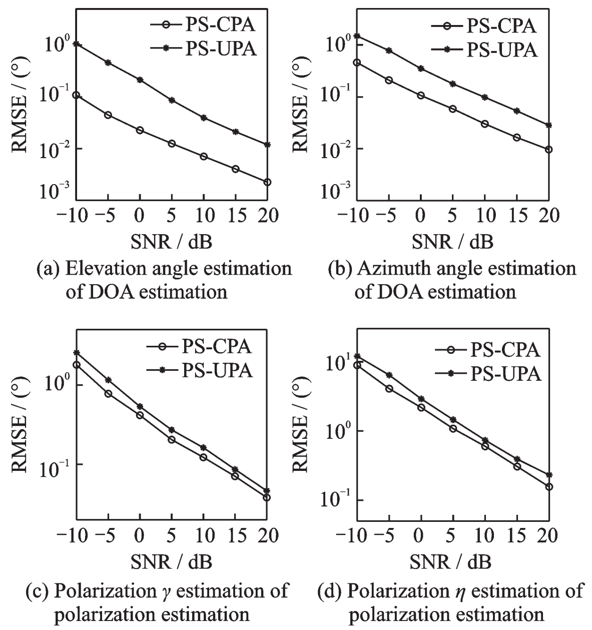

(a) Elevation angle estimation of DOA estimation

(b) Azimuth angle estimation of DOA estimation

(c) Polarization γ estimation of polarization estimation

(d) Polarization η estimation of polarization estimation

Fig.7 Parameter estimation performance of different arrays

5 Conclusions

This paper focuses on PS-CPAs and proposes a fast-convergence quadrilinear decomposition approach for DOA and polarization estimation with the PS-CPAs. To accelerate convergence of the conventional quadrilinear decomposition algorithm, the proposed approach first employs PM as the initialization, and then arranges the receive data into two quadrilinear models to perform QALS. Thereafter, the phase ambiguity can be eliminated and the polarization estimates paired with DOA can be achieved by utilizing the previous estimations. Simulations demonstrate the superiority of the proposed approach in terms of computational complexity and estimation performance.

References

[1] TSANG L, KONG J A, DING K H. Scattering of electromagnetic waves: Theories and applications[M]. Boston, USA: John Wiley & Sons, 2004.

[2] ZHANG X F, WANG F, XU D Z. Theory and application of array signal processing[M]. Beijing: National Defence Industry Press, 2013.

[3] WONG K T, ZOLTOWSKI M D. Closed-form direction finding and polarization estimation with arbitrarily spaced electromagnetic vector-sensors at unknown locations[J]. IEEE Transactions on Antennas & Propagation, 2000, 48(5): 671-681.

[4] ZHANG X, SHI Y, XU D. Novel blind joint direction of arrival and polarization estimation for polarization-sensitive uniform circular array[J]. Progress in Electromagnetics Research, 2008, 86: 19-37.

[5] LI S, ZHANG X F, WANG F. CS quadrilinear model-based angle estimation for MIMO radar with electromagnetic vector sensors[J]. International Journal of Electronics, 2016, 104(3): 485-503.

[6] ZHANG X F, CHEN C, LI J, et al. Blind DOA and polarization estimation for polarization-sensitive array using dimension reduction MUSIC[J]. Multidimensional Systems and Signal Processing, 2014, 25(1): 67-82.

[7] LI J, COMPTON R T. Two-dimensional angle and polarization estimation using the ESPRIT algorithm [J]. IEEE Transactions on Antennas & Propagation, 1992, 40(5): 550-555.

[8] VAIDYANATHAN P P, PAL P. Sparse sensing with co-prime samplers and arrays[J]. IEEE Transactions on Signal Processing, 2011, 59(2): 573-586.

[9] ZHOU C, SHI Z, GU Y, et al. DECOM: DOA estimation with combined MUSIC for coprime array[C]// Proceedings of the 2013 International Conference on Wireless Communications and Signal Processing. Hangzhou, China: IEEE, 2013: 1-5.

[10] WU Q, SUN F, LAN P, et al. Two-dimensional direction-of-arrival estimation for co-prime planar arrays: A partial spectral search approach[J]. IEEE Sensors Journal, 2016, 16(14): 5660-5670.

[11] ZHENG W, ZHANG X F, SHI Z. Two-dimensional direction of arrival estimation for coprime planar arrays via a computationally efficient one-dimensional partial spectral search approach[J]. IET Radar, Sonar & Navigation, 2017, 11(10): 1581-1588.

[12] COSTA J P C L D, ROEMER F, HAARDT M, et al. Multidimensional model order selection[J]. EURASIP Journal On Advances In Signal Processing, 2011 (1): 1-13.

[13] NION D, SIDIROPOULOS N D. Adaptive algorithms to track the PARAFAC decomposition of a third-order tensor[J]. IEEE Transactions on Signal Processing, 2009, 57(6): 2299-2310.

[14] LI J, ZHANG X. Joint estimation of angle and Doppler frequency in bistatic MIMO radar based on quadrilinear decomposition[J]. Acta Aeronautica et Astronautica Sinica, 2012, 33(8): 1474-1482.

[15] LI J, ZHANG X, CHEN H. Improved two-dimensional DOA estimation algorithm for two-parallel uniform linear arrays using propagator method[J]. Signal Processing, 2012, 92(12): 3032-3038.

[16] XU L, WU R H, ZHANG X F. Joint two-dimensional DOA and frequency estimation for L-shaped array via compressed sensing PARAFAC method[J]. IEEE Access, 2018, 6: 37204-37213.

[17] STOICA P, NEHORAI A. Performance study of conditional and unconditional direction-of-arrival estimation[J]. IEEE Transactions on Acoustics, Speech, and Signal Processing, 1990, 38(10): 1783-1795.

Acknowledgement This work was supported by the Open Research Fund of the State Key Laboratory of Complex Electromagnetic Environment Effects on Electronics and Information System (No.CEMEE2019Z0104B).

Authors Dr. **XU Xiong** is a research assistant of the State Key Laboratory of Complex Electromagnetic Environment Effects (CEMEE) on Electronic and Information System. He got his Ph.D. degree from University of Electronic Science and Technology of China (UESTC) in 2012. His research interests include Signal Processing and Machine Learning.

Prof. **ZHANG Xiaofei** received his M.S. degree from Wuhan University in 2001 and Ph.D. degree in communication and information systems from Nanjing University of Aeronautics and Astronautics in 2005. He is now a full professor at College of Electronic and Information Engineering of Nanjing University of Aeronautics and Astronautics. His research is focused on array signal processing and communication signal processing.

Author contributions Dr. **XU Xiong** designed the study and analyzed the performance. Ms. **SHEN Jinqing** provided the simulation results and wrote the manuscript. Mr. **ZHU Beizuo** contributed to the discussion and background. Prof. **ZHANG Xiaofei** provided guidance of the study.

Competing interests The authors declare no competing interests.

(Production Editor: ZHANG Bei)

极化敏感面阵波达方向和极化的联合估计-快速收敛四线性分解算法

许 雄[1],沈金清[1,2],朱倍佐[1,2],张小飞[1,2]

(1. 电子信息系统复杂电磁环境效应国家重点实验室,洛阳 471003, 中国;
2. 南京航空航天大学电子与信息工程学院,南京 211106, 中国)

摘要:调查了极化面阵中的波达方向估计(Direction of arrival,DOA)与极化估计问题,并提出了一种快速收敛的四线性分解算法。具体来说,首先把互质面阵分解为两个均匀面阵并利用传播算子算法得到了初始的方向矩阵估计。然后,将接受信号置于四线性模型,利用四线性交替最小二乘来估计所有可能的DOA与极化估计结果。接着,根据互质解模糊的原理,从所有的结果中提取出真正的估计值,消除了模糊估计结果。对比于传统的四线性交替最小二乘算法,本算法可以在不损失估计性能的前提下,极大程度地降低复杂度。仿真结果证明了极化互质面阵下本快速收敛算法的优越性。

关键词:极化敏感阵列;互质面阵;波达方向估计;极化估计;四线性分解;快速收敛